VTT Technical Research Centre of Finland

Validation of the Ants-TRACE code system with VVER-1000 coolant transient benchmarks

Lauranto, Unna; Komu, Rebekka; Rintala, Antti; Valtavirta, Ville

Published in:
Annals of Nuclear Energy

DOI:
10.1016/j.anucene.2023.109879

Published: 15/09/2023

Document Version
Publisher's final version

Annals of Nuclear Energy 190 (2023) 109879

Contents lists available at ScienceDirect

Annals of Nuclear Energy

journal homepage: www.elsevier.com/locate/anucene

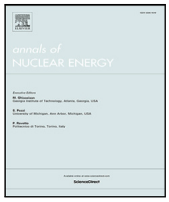

Validation of the Ants-TRACE code system with VVER-1000 coolant transient benchmarks

Unna Lauranto *, Rebekka Komu, Antti Rintala, Ville Valtavirta

VTT Technical Research Centre of Finland Ltd, P.O. Box 1000, FI-02044 VTT, Finland

ARTICLE INFO

Keywords:
Ants
TRACE
VVER-1000
Coolant transient
Coupled calculation
Kraken

ABSTRACT

The objective of this paper is to start the validation of the coupled code system of the nodal neutronics solver Ants and the system code TRACE. The process consists of two exercises of well-known VVER-1000 coolant transient benchmarks: a core-vessel simulation of a main steam line break transient of the V1000CT-2 benchmark and a full plant simulation of a main coolant pump trip of the Kalinin-3 benchmark. The Ants-TRACE results are compared against other code solutions in the V1000CT-2 benchmark and measurement data in the Kalinin-3 benchmark. The results show good agreement in both benchmarks, with the deviations ranging mostly within the measurement error or the range of deviations of other published solutions. The results confirm the correct implementation of the coupling and successful modeling of relevant phenomena in coolant transient events in a VVER-1000 reactor.

1. Introduction

VTT is currently making a total renewal of its computational tools for nuclear safety analyses. The in-house legacy codes developed since the 70's for safety analyses of the Finnish nuclear power plants no longer serve the purpose of modeling modern technologies, such as small modular reactors and advanced reactors. In order to fulfill the needs of modeling modern reactor technologies, a new computational framework called Kraken has been developed at VTT since 2017 (Leppänen et al., 2022). The aim of Kraken is to perform coupled core physics calculations for safety analyses, including transient events. Previously conducted with the HEXTRAN-SMABRE code system (Kyrki-Rajamäki, 1995), the core-plant transient scenarios for VVER-type reactors are intended to be performed with a coupled code system of VTT's nodal neutronics solver Ants (Sahlberg and Rintala, 2018) and system code TRACE (U. S. Nuclear Regulatory Commission, 2020). So far, Ants has been used in steady-state and burnup modeling of different reactor types. Rintala and Lauranto (2022) presented the recently-implemented time-dependent model of Ants. TRACE is a well-established system code and has been widely used in nuclear safety applications. The coupling between Ants and TRACE has been implemented recently by Tuominen et al. (2022). The aim of this work is to start the validation of Ants-TRACE using well-known VVER-1000 transient benchmarks, the V1000CT-2 and the Kalinin-3 coolant transient benchmarks.

2. Methods

2.1. Kraken

A new computational framework called Kraken is currently under development at VTT Technical Research Centre of Finland. The aim of Kraken is to perform deterministic safety analyses with coupled core physics calculations. Additionally, Kraken can be utilized as the main tool in reactor design process (Leppänen et al., 2021). Recently, Kraken has been applied to different problems for validation and verification, though the verification process has been conducted mostly for individual solvers. However, the verification of coupled code systems has started with coupled fuel cycle simulations.

Kraken enables coupling of multiple in-house modular solvers representing different fields of physics in a reactor. Kraken is built around VTT's Monte Carlo transport code Serpent (Leppänen et al., 2015), which can produce high-fidelity neutronics solutions. In addition to the high-fidelity option, Serpent can be used in the two-step calculation chain to perform group constant generation for the nodal neutronics solver Ants for computationally lighter reduced-order neutronics. The fuel mechanics of the Kraken framework is solved by SuperFINIX (Valtavirta et al., 2019) and thermal-hydraulics of the core is solved by Kharon. The communication between the solvers is conducted by the multiphysics driver Cerberus. Kraken can also be coupled to system-level codes, such as Apros (Apros, 2022) and TRACE to perform plant-level calculations. This work uses the Ants-TRACE code coupling in the Kraken framework.

* Corresponding author.
E-mail address: unna.lauranto@vtt.fi (U. Lauranto).

https://doi.org/10.1016/j.anucene.2023.109879
Received 9 December 2022; Received in revised form 14 March 2023; Accepted 17 April 2023
Available online 28 April 2023

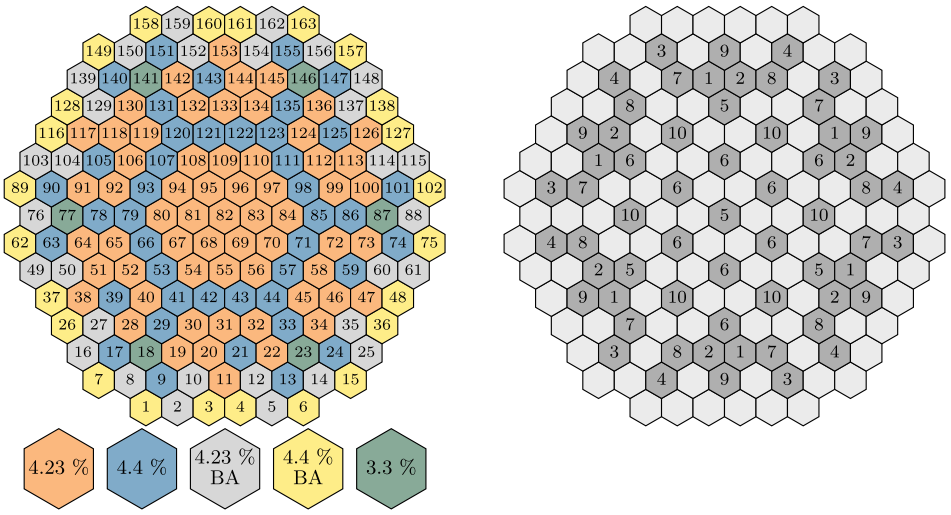

(a) Fuel assembly numbering and types. (b) Control rod group numbering.

Fig. 1. VVER-1000 core radial layout in the V1000CT-2 benchmark. The fuel assembly types indicate the U-235 enrichment in percentages and the presence of burnable absorbers as BA.

2.2. Ants

Ants is a nodal neutronics solver developed at VTT since 2017. Ants is capable of solving steady-state, transient and burnup problems. The methodology of Ants is based on solving the multi-group diffusion equation by applying the analytic function expansion nodal (AFEN) (Woo et al., 2001) and function expansion nodal methods (FENM) (Xia et al., 2006). Ants supports rectangular, hexagonal and triangular geometries, and is thus applicable for any type of pressurized water reactor (PWR) geometry. The Ants steady-state methodologies with the different geometries are presented in detail by Sahlberg and Rintala (2018), Rintala and Sahlberg (2019) and Hirvensalo et al. (2021). The transient capability of Ants has been implemented and demonstrated recently by Rintala and Lauranto (2022).

2.3. TRACE

TRACE (TRAC/RELAP Advanced Computational Engine) is a thermal-hydraulic system code by the U.S. Nuclear Regulatory Commission (NRC) widely used for nuclear safety applications (U. S. Nuclear Regulatory Commission, 2020). It can be used for modeling accidents and transients in both pressurized and boiling water reactors. TRACE is capable of modeling both 1D and 3D thermal-hydraulic (TH) phenomena alone or together coupled with a reactor physics code. TRACE utilizes a component-based approach to model reactor systems. Version 5 Patch 6 of TRACE is used in this work.

2.4. Ants-TRACE coupling

In the Ants-TRACE coupling, Ants solves the 3D core power distribution and TRACE solves the system thermal-hydraulics. The power density field is transferred from Ants to the TRACE fuel heat structures. TRACE solves the fuel temperature and heat transfer to coolant. Fuel temperature and coolant temperature and density are then transferred to Ants. The spatial mappings between Ants and TRACE heat structures and fluid components are provided in separate files and are case-dependent.

In the explicit coupling, the time step size is determined by TRACE. At first, Ants calculates the initial power distribution based on the initial TH conditions. TRACE then calculates the first time step based on the Ants power distribution. The time step size and other data at the end of the time step are transferred to Ants. The power distribution is then updated based on that state and given to TRACE. This loop is repeated until the end criterion is met. The calculation flow is similar in both steady-state and transient calculations. The user can decide to update the Ants solution either in every time interval or only in certain time intervals. In coupled transient calculation, three calculation steps are required: steady-state TRACE, steady-state Ants-TRACE and transient Ants-TRACE.

3. Benchmark descriptions

3.1. VVER-1000 coolant transient benchmark V1000CT-2

Phase 2 of the VVER-1000 coolant transient benchmark (V1000CT-2) was first introduced in 2006 by OECD/NEA (Kolev et al., 2006). It describes coolant mixing experiments and a hypothetical main steam line break (MSLB) transient in the Kozloduy-6 nuclear power plant (NPP) unit. The calculations of this work include Exercise 2 of the benchmark, in which a coupled core-vessel simulation with the given MSLB boundary conditions is conducted.

The VVER-1000 reactor core consists of 163 hexagonal fuel assemblies of five different types. The assembly types have one of three different uniform enrichments and either contain or do not contain burnable absorber in some fuel rods. There are 10 control rod groups present in the core. The core radial layout and control rod groups are shown in Fig. 1.

Exercise 2 of the benchmark includes two different transient scenarios. In both scenarios, the main steam line break occurs in loop 4 followed by a scram signal. Scenario 1 is a realistic scenario of the MSLB event including main coolant pump (MCP) trip of the faulted loop. In this scenario, the scram worth is sufficient for maintaining reactor shutdown after scram. In Scenario 2, the MCP of the faulted loop fails to trip, which results in all the MCPs remaining in operation. The overcooling of the core together with reduced scram worth of the control rods causes the reactor to return to power after scram.

In the initial state of the transient, the reactor is at the end-of-cycle (EOC) with a fuel burnup of 270.4 EFPD. Group constants are given in the benchmark for fuel, control rod and reflector nodes. The group constants include diffusion coefficients and macroscopic scattering, absorption and fission cross sections. The group constants are given as a function of moderator density and fuel temperature. Two separate sets of control rod group constants are given for the two scenarios.

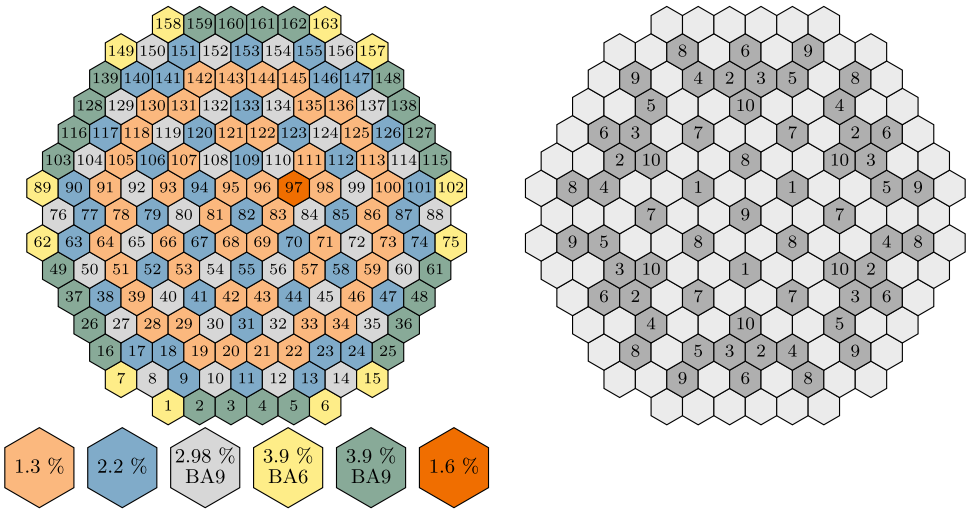

(a) Fuel assembly numbering and types. (b) Control rod group numbering.

Fig. 2. VVER-1000 core radial layout in the Kalinin-3 benchmark. The fuel assembly types indicate the U-235 enrichment in percentages, and the presence and number of burnable absorber rods as BA.

For Scenario 2, the absorption cross sections of the control rods are modified.

The thermal-hydraulic boundary conditions for the reactor pressure vessel are also given in the specifications. The boundary conditions include coolant temperatures and mass flow rates at the vessel inlets, and pressure at the outlets.

3.2. Kalinin-3 coolant transient benchmark

Kalinin-3 coolant transient benchmark (Tereshonok et al., 2009) was published in 2008 as a continuation to the V1000CT benchmarks. The benchmark scenario describes a real main coolant pump switch-off experiment in the Kalinin NPP unit 3. This work includes Exercise 3 of the benchmark, in which a coupled core-plant transient is modeled. The transient is initiated with a switch-off of the MCP of loop 1 at nominal power. The switch-off is followed by control rod movement to reduce the power level to 67.2%.

The Kalinin-3 unit is mostly identical to the Kozloduy-6 unit. However, the five different assembly types and control rod groups differ from the V1000CT-2 benchmark. The core layout and control rod groups of the Kalinin-3 core are shown in Fig. 2. The fuel is at 96 EFPD burnup with the exception of one assembly with fresh fuel in the core at position 97. The group constants of this problem were given in the benchmark specifications for fuel, reflector and control rod nodes. The group constants consist of diffusion coefficients and macroscopic cross sections as a function of fuel temperature, moderator temperature and moderator density. To account for the assembly replaced with fresh fuel, the 60° sector of the core where the fresh fuel assembly is located, has a separate set of group constants.

4. Ants-TRACE model

The original VVER-1000 input for TRACE was received from Karlsruhe Institute of Technology in 2019. The model components and nodalization are presented in Fig. 3. It has since been modified for the coolant transients. The model is comprised of the reactor pressure vessel, primary circuit, and secondary circuit all the way to the turbine valves including the necessary control systems. The model was simplified for the V1000CT-2 Exercise 2 so that it includes only the reactor pressure vessel with boundary conditions at cold legs and hot legs. This allows testing the coupling without any unnecessary disturbances from the system side.

The TRACE VVER-1000 model utilizes a cylindrical 3D VESSEL component for the reactor pressure vessel. It has six sectors and six radial rings. The core comprises of three radial rings for the active core and one ring for the radial reflector. The core includes 30 uniform axial levels for the active rod length and additional levels for top and bottom reflectors. Fig. 4(a) shows the nodalization for the core area in TRACE. 24 heat structures represent the fuel assemblies and radial reflector with the same axial division. The Ants input has one radial node per fuel assembly and 32 axial nodes as shown in Fig. 4(b). The reflector region is characterized radially with one layer of nodes with similar radial dimensions in the outer peripheries of the core. The radial mapping scheme between Ants and TRACE is presented in Fig. 5 with the single fuel assemblies representing Ants nodes and the different colors representing TRACE nodes. The center node is divided between the six sectors. In reality, the core is rotated six degrees clockwise in relation to the loops, and the sector division of the TRACE model was based on that. Axially there is a one-to-one correspondence between the codes.

5. Results

This section provides the Ants-TRACE results of both coolant transient benchmarks. The steady-state results of the initial state as well as time histories of various parameters during the transient are presented. The calculation scheme for both benchmark problems consists of a stand-alone TRACE steady-state calculation of the initial state, a coupled Ants-TRACE steady-state calculation of the initial state and finally the coupled transient calculation with Ants-TRACE. Both benchmarks were calculated with zero flux neutronics boundary conditions applied in the core periphery. The time steps were set automatically by TRACE and the time step was approximately 7.5 ms. In both problems, the group constants given in the specifications were applied in the calculations.

5.1. VVER-1000 coolant transient benchmark V1000CT-2 results

In V1000CT-2 benchmark Exercise 2, the Ants-TRACE results are compared against VTT's legacy code HEXTRAN-SMABRE. HEXTRAN-SMABRE has been thoroughly validated and used in analyses of VVER-type reactors (Syrjälahti and Hämäläinen, 2006). The HEXTRAN-SMABRE results of this benchmark were published in the benchmark results among other code systems (Kolev et al., 2006).

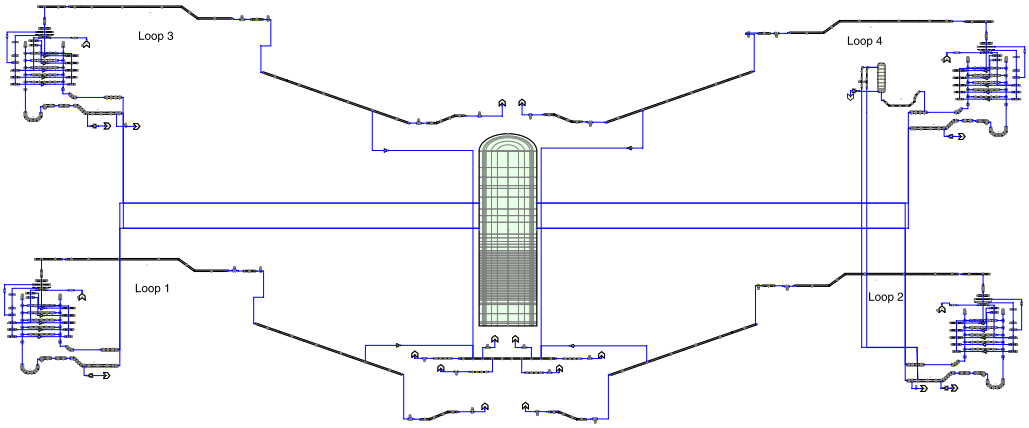

Fig. 3. VVER-1000 model for TRACE.

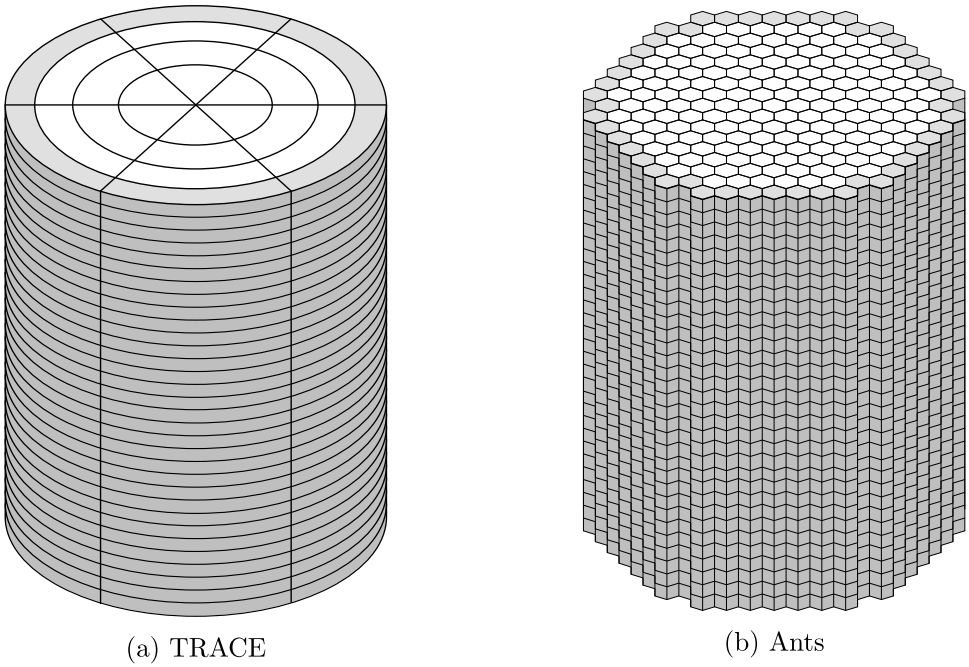

Fig. 4. Nodalization for the core area in TRACE and Ants. Reflector nodes are marked with gray.

5.1.1. Steady-state results

The computed parameters of the initial state calculated with Ants-TRACE are presented in Table 1. The table also shows results by HEXTRAN-SMABRE and the average of the solutions by the codes given in the benchmark. The Ants-TRACE value for the effective multiplication factor k_{eff} has good agreement in comparison to the other solutions and the value fits in the range of the deviations of other code solutions. Ants-TRACE gives the highest value in the power peaking factor in the radial direction (F_{xy}) compared to the other codes. However, the deviation from the average solution is only 1.4%, which can be considered acceptable. The peaking factor in the axial direction (F_z) is within the same range as the other nodal codes.

The Ants-TRACE radial power distribution of the initial state normalized to unity is shown in Fig. 6. The absolute differences to the corresponding power distribution calculated with HEXTRAN-SMABRE are shown in Fig. 7. In the initial state, all control rod groups are fully withdrawn with the exception of control rod group 10, which is 20 % inserted. The largest differences between the code solutions occur in the periphery of the core. The largest negative deviation is −0.104 and the maximum positive deviation is 0.08. On average, the two solutions deviate by 0.05 and the root-mean-square (RMS) difference is 5.79%.

Table 1
Computed parameters of the initial state of the V1000CT-2 transient.

Code	k_{eff}	F_{xy}	F_z
Ants-TRACE	0.99632	1.311	1.141
HEXTRAN-SMABRE	1.00210	1.303	1.187
Average of reference codes	0.99831	1.293	1.169
Min/max of reference codes	0.99481/1.00210	1.279/1.303	1.139/1.187

The Ants-TRACE relative axial power distribution in the initial state of the transient is presented in Fig. 8 together with the solution calculated with HEXTRAN-SMABRE. In addition, an average axial power distribution based on five different code solutions given in the benchmark results (Kolev et al., 2010) is presented. Axial nodalization of 30 nodes is utilized in all solutions. As shown in the figure, the

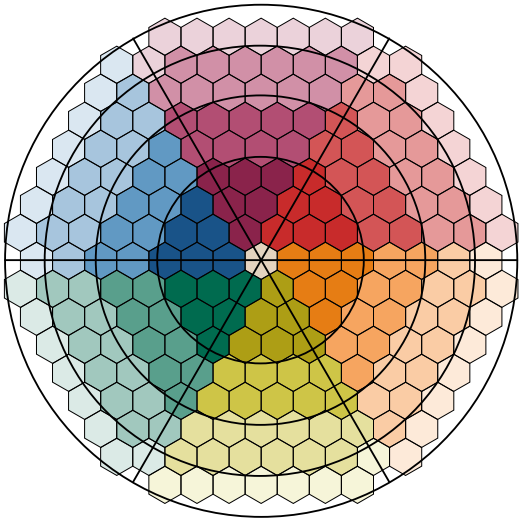

Fig. 5. Radial coupling scheme between the Ants and TRACE inputs. The coloring of the hexagonal Ants nodes indicates the mapping to each TRACE node.

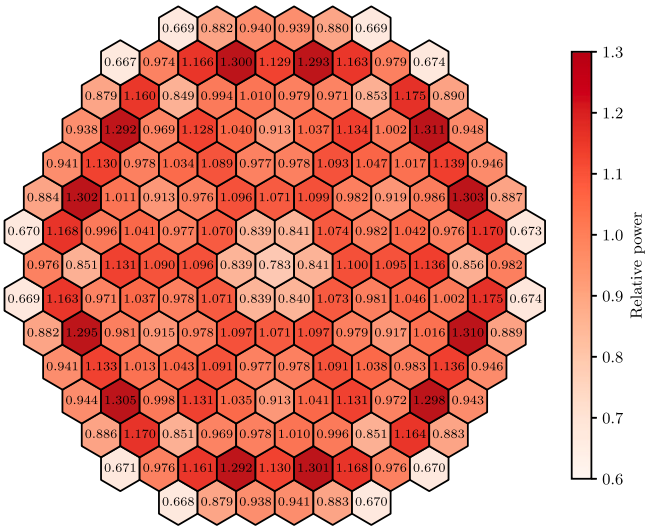

Fig. 6. Ants-TRACE relative radial power distribution in the initial state of the V1000CT-2 transient.

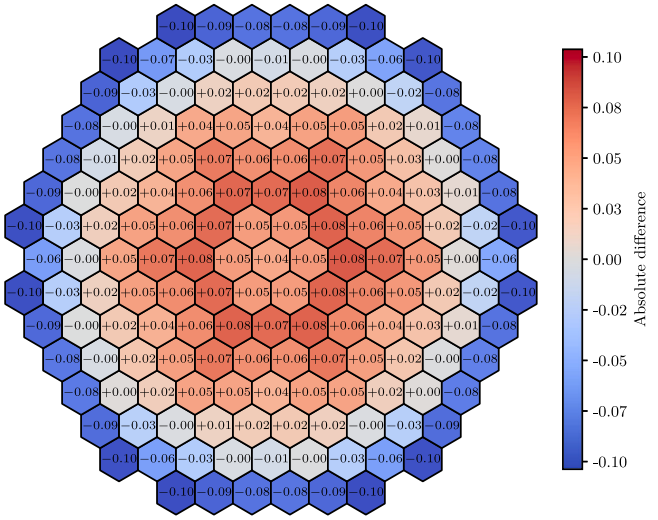

Fig. 7. Absolute difference between the radial power distributions of Ants-TRACE and HEXTRAN-SMABRE in the initial state of the V1000CT-2 transient.

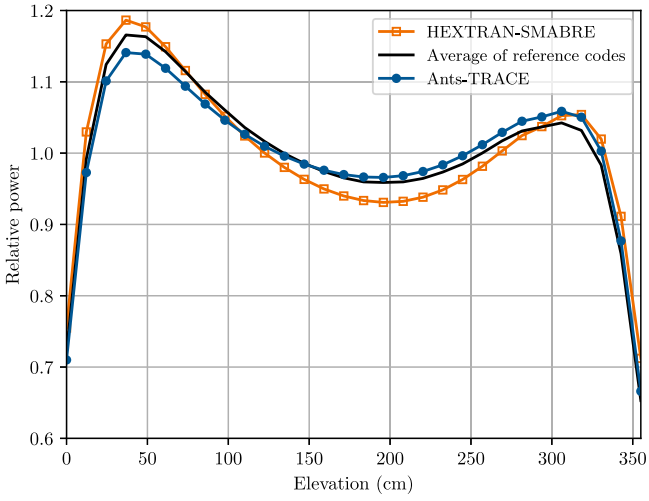

Fig. 8. Relative axial power distribution in the initial state of the V1000CT-2 transient.

Ants-TRACE solution deviates from the average solution in the same range as HEXTRAN-SMABRE. The Ants-TRACE solution has a RMS error of 1.5% compared to the average solution. The corresponding value of the HEXTRAN-SMABRE solution is 2.5%. The differences in the Ants-TRACE and HEXTRAN-SMABRE results are based on the different neutronics solution methodologies in the codes. In addition, the reflector modeling in HEXTRAN is conducted by single-state albedos, whereas Ants models the reflector nodes individually and includes feedback effects in the reflector nodes as well.

5.1.2. Transient results

The transient in the V1000CT-2 benchmark is initiated with a MSLB event in loop 4. The event causes asymmetric overcooling in the core. In Scenario 1, the MCP of loop 4 trips and scram is initiated with one stuck rod at assembly 90. The stuck rod is positioned in the sector of the faulted loop. Fission power during the Scenario 1 transient is shown in Fig. 9(a).

Scenario 2 of the benchmark describes a pessimistic alternative to Scenario 1. In this scenario, the MCP4 fails to trip, which causes stronger overcooling in the core. In addition, the scram worth of the control rods is reduced and two stuck rods at positions 117 and 140 are present in the sector of the faulted loop. The overcooling and reduced scram worth cause the reactor to return to power after scram, as shown in Fig. 9(b). The agreement between Ants-TRACE and HEXTRAN-SMABRE is especially good in Scenario 1. In Scenario 2, the return to power due to negative reactivity feedbacks is modeled with Ants-TRACE successfully. Some deviations occur between Ants-TRACE and HEXTRAN-SMABRE as well as other codes shown in the benchmark due to the difficult nature of the phenomenon.

Mass flow rate and cold leg (CL) temperature boundary conditions in both scenarios are shown in Figs. 10 and 11. The calculated hot leg (HL) temperatures compared to HEXTRAN-SMABRE are presented in Fig. 12. In Scenario 1, the HL4 temperature is given as a boundary condition, because the flow in loop 4 is reversed. Stronger overcooling can be seen in Scenario 2, as the pump in the faulted loop is not tripped. There is a good agreement between the Ants-TRACE and HEXTRAN-SMABRE results.

In scenario 2, the power peaks at 69 s during maximum overcooling. The Ants-TRACE radial power distribution at the time of the power peak is shown in Fig. 13. The absolute differences to the corresponding power distribution calculated with HEXTRAN-SMABRE are shown in Fig. 14. The power peaks at the sector with most cooling near the

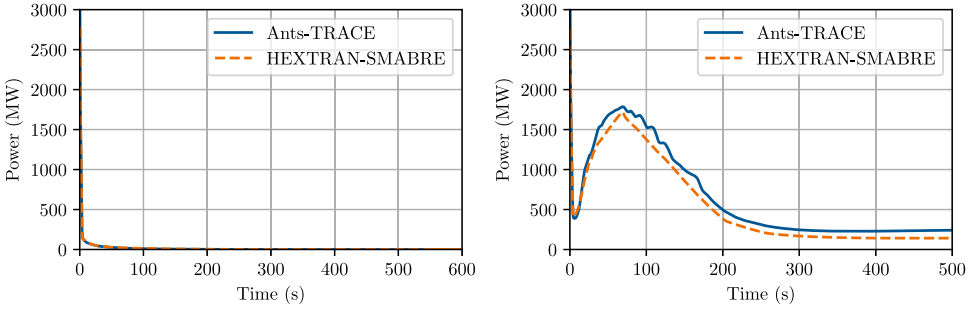

Fig. 9. Fission power during the V1000CT-2 MSLB transient.

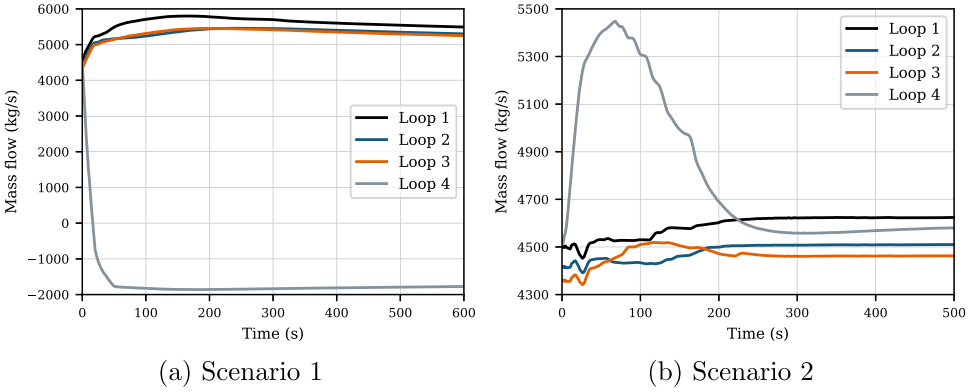

Fig. 10. Loop mass flow rates during the V1000CT-2 MSLB transient.

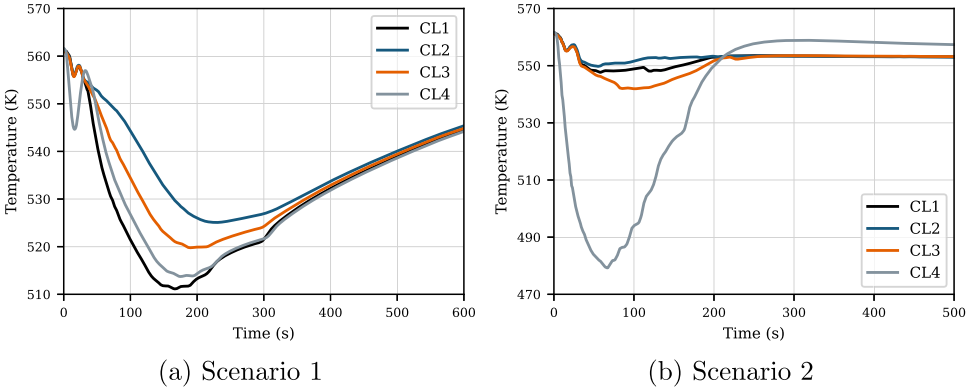

Fig. 11. Cold leg temperatures during the V1000CT-2 MSLB transient.

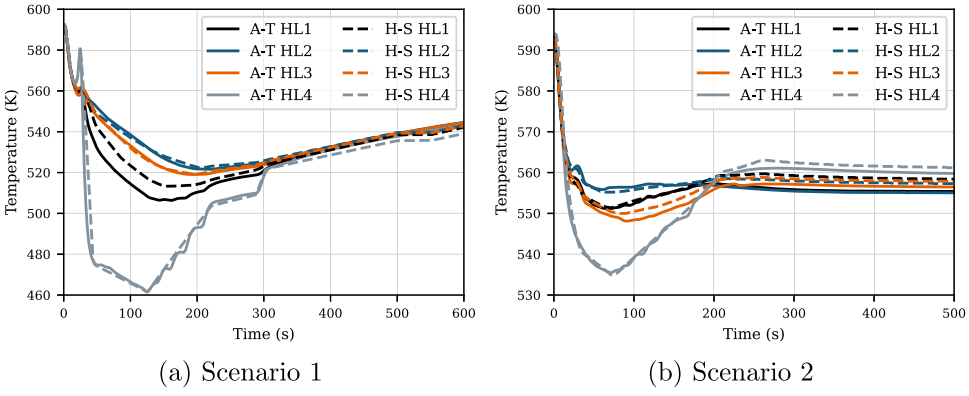

Fig. 12. Hot leg temperatures during the V1000CT-2 MSLB transient.

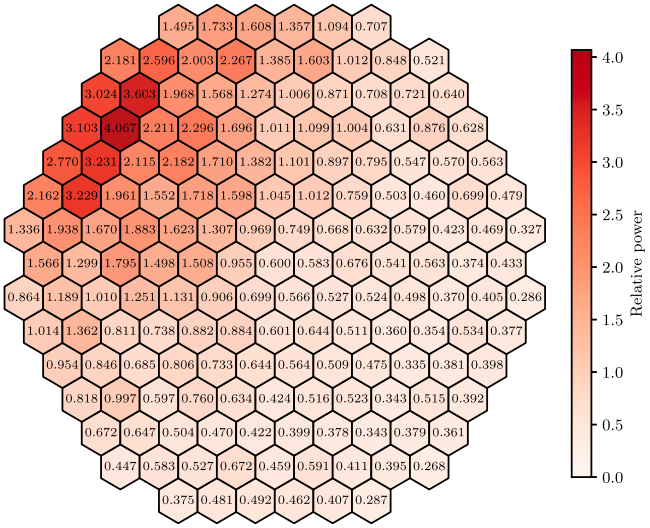

Fig. 13. Ants-TRACE relative radial power distribution at highest return to power (69 s) in Scenario 2 of the V1000CT-2 transient.

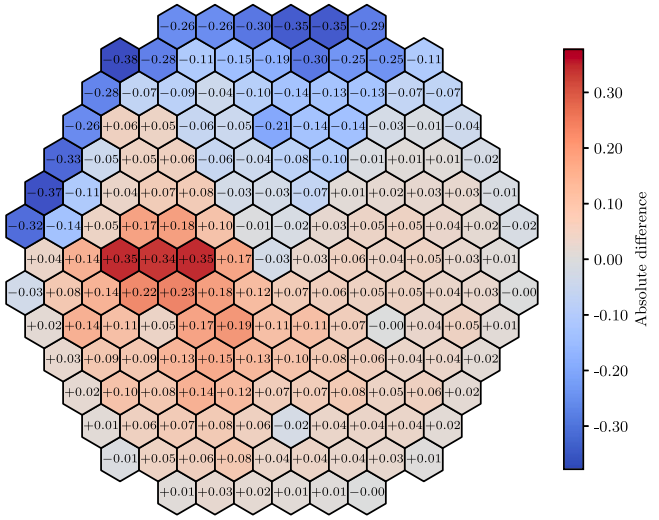

Fig. 14. Absolute difference between the radial power distributions of Ants-TRACE and HEXTRAN-SMABRE at highest return to power (69 s) in Scenario 2 of the V1000CT-2 transient.

two stuck rods. The differences to the HEXTRAN-SMABRE solution are significant in parts. The average deviation is 0.09 and the RMS difference is 13.28%.

The largest differences between Ants-TRACE and HEXTRAN-SMABRE occur in the vicinity of the sector of the faulted loop. The maximum deviation of −0.38 occurs in the periphery of the core, where the power is peaked. As the differences are given as absolute differences, the large deviations in the high power assemblies are expected. The largest positive difference of 0.35 occurs at the border of the TRACE sector. The reason to the differences lies in the sector divisions of TRACE and SMABRE. Both have six sectors, but the fuel assemblies are assigned to the sectors differently, which contributes to larger differences on the edges of the sectors. In particular, the nodes showing the maximum differences in Fig. 14 are included in different sectors in TRACE and SMABRE, which affects the coolant mixing and therefore temperature in those nodes. In TRACE, the specific nodes are part of the upper sector, in which the cooling is more pronounced. As the upper sector is the sector where the overcooling occurs, the assembly powers are higher. In SMABRE however, the same nodes belong to the lower sector, in which the cooling is less significant. In addition, HEXTRAN includes decay heat as opposed to Ants, which affects to the differences in the power distributions. The large differences in the assembly power distribution at the time of the power peak are apparent in the benchmark results (Kolev et al., 2010) between other codes as well.

The axial power distributions of Ants-TRACE and HEXTRAN-SMABRE at 69 s are shown in Fig. 15. The agreement is relatively good, with the RMS difference between the codes of 2.8%.

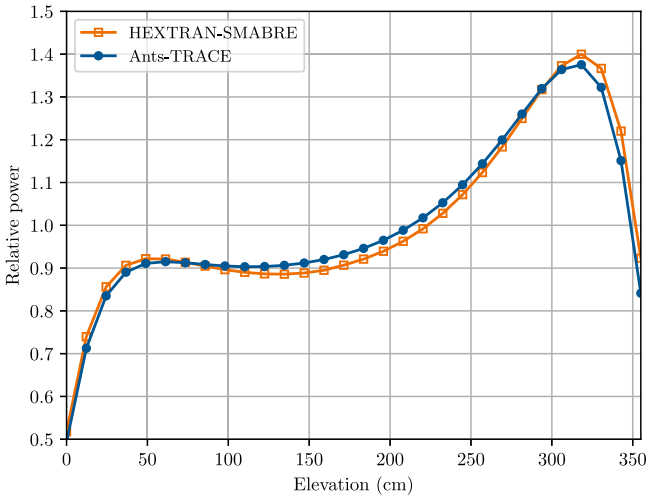

Fig. 15. Relative axial power distribution at highest return to power (69 s) in Scenario 2 of the V1000CT-2 transient.

5.2. Kalinin-3 coolant transient benchmark results

The Ants-TRACE results of Kalinin-3 benchmark Exercise 3 are compared to actual measured data provided in the benchmark (Tereshonok et al., 2009).

5.2.1. Steady-state results

The initial state of the Kalinin-3 transient is at nominal power with control rod group 10 inserted 82.95% from the bottom of the core and all other control rods withdrawn. The Ants-TRACE radial power distribution in the initial state is shown in Fig. 16. The assembly powers are normalized to unity. The relative difference between Ants-TRACE results and measurements is shown in Fig. 17. The average deviation from the experimental results is 1.53% and the RMS error is 1.89%. The maximum difference of 5.49% occurs at assembly position 97, which is the position with the original fuel assembly replaced to a fresh fuel assembly. The relative differences of the radial power distribution are within the measurement uncertainty of 5 % for the ICMS (in-core measurement system) (Georgieva, 2016), with the exception of the fresh fuel assembly, which exceeds the limit only slightly. The axial power distribution in the initial state is shown in Fig. 18. Experimental results were available for six axial points also shown in the figure. With the axial power normalized to unity, the agreement between Ants-TRACE power and the experimentally obtained power is very good.

5.2.2. Transient results

The Ants-TRACE total power and control rod movements during the Kalinin-3 MCP switch-off transient are shown in Fig. 19. The experimentally obtained reference data is shown in the figure as well. The transient is initiated at the switch-off of MCP1 at 0 s. At 1.41 s, the control rod group 10 is inserted inwards. Control rod group 9 is also inserted momentarily. The reactor is stabilized at a lower power

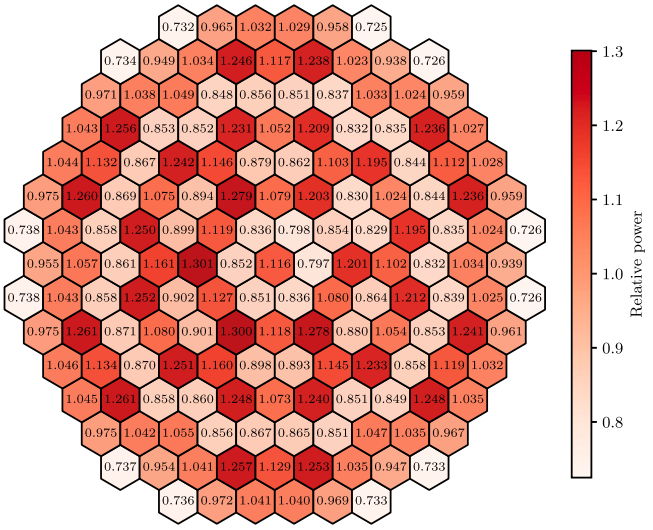

Fig. 16. Ants-TRACE relative radial power distribution in the initial state of the Kalinin-3 transient.

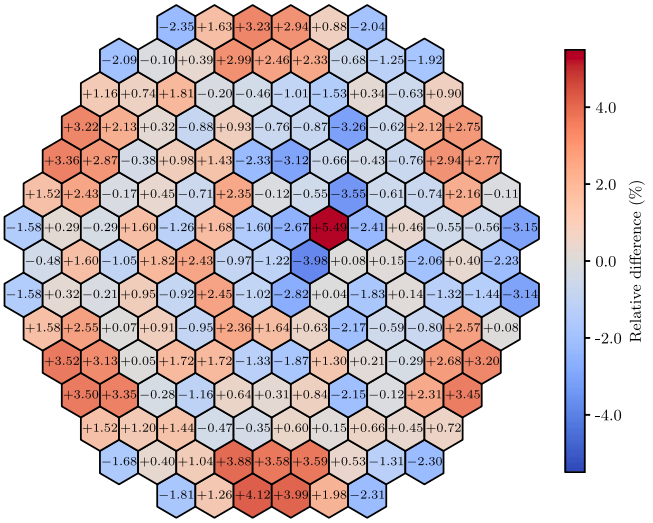

Fig. 17. Relative difference between the radial power distributions of Ants-TRACE and measured data in the initial state of the Kalinin-3 transient.

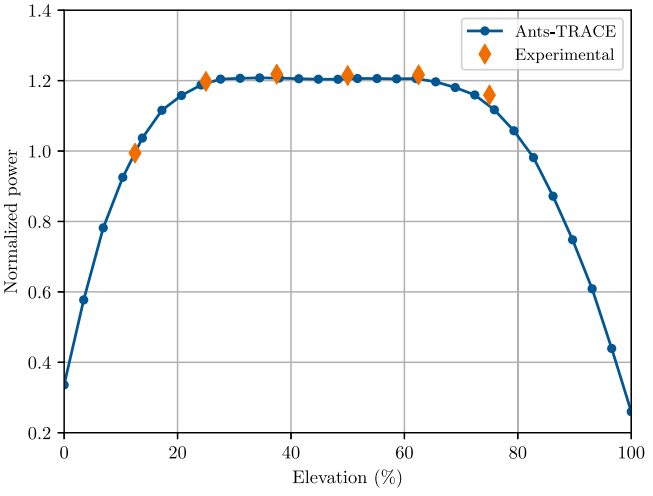

Fig. 18. Relative axial power distribution in the initial state of the Kalinin-3 transient.

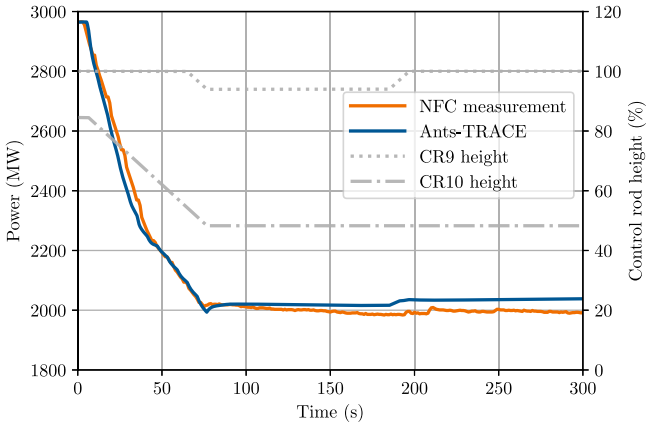

Fig. 19. Total power during the Kalinin-3 transient.

level when the control rod movement stops. The experimental data is measured in the reactor by the neutron flux control system (NFC). Considering the measurement error of power of 60 MW in nominal power (Ivanov et al., 2002), the agreement between the Ants-TRACE solution and the experimental results is very good.

Loop mass flow rates compared to measurements and MCP rotational speeds are presented in Figs. 20(a) and 20(b). The flow in loop 1 is reversed at 20 s and the pump stops at 55 s. The flow in other loops is slightly increased. The loop 1 mass flow rate measurement has discontinuity caused by the change in mass flow rate estimation algorithm as the flow is reversed, which makes the measurement unreliable for the first 90 s of the transient (Georgieva, 2016). Apart from that, the measurement uncertainty is ±200 kg/s (Ivanov et al., 2002). At the initial state, the differences between the Ants-TRACE results and measurements are less than 100 kg/s, but at the end of the transient they are 170–280 kg/s, which in some loops is slightly larger than the measurement error.

Cold and hot leg temperatures compared to measurements are shown in Figs. 20(c) and 20(d). Hot leg 1 temperature decreases as the flow is reversed and the cold leg 1 temperature fluctuates. The calculated values are taken from pipe nodes, which are closest to the measurement location. Time delay of the temperature measurements is not taken into account in the comparison. The measurement uncertainty is ±2 K (Ivanov et al., 2002). The Ants-TRACE results are in relatively good agreement with the measurements and within the uncertainty bounds. Filtering the results with a time constant would move the calculated peaks closer to the measured ones.

The Ants power distribution at the end of the transient (300 s) is shown in Fig. 21. The power distribution is relatively symmetric, with the exception of the fresh fuel assembly, in which the power is lower compared to other symmetric positions. The corresponding relative differences to measured values are shown in Fig. 22. The maximum difference of 6.50% occurs in the periphery of the core. In the position of the fresh fuel assembly, the difference is also large in comparison to surrounding assemblies. The average deviation from the measured values is 1.76% and the RMS error is 2.23%. The maximum differences exceed the measurement error of 5 % slightly.

The axial power distributions of Ants-TRACE and the experimental values at the end of the transient at 300 s are shown in Fig. 23. The agreement with the six experimental data points is relatively good.

6. Conclusions

The Ants-TRACE coupling was tested for the first time in large-scale with two VVER-1000 coolant transient benchmarks. First, Exercise 2 of the V1000CT-2 benchmark, consisting of a core-vessel main steam

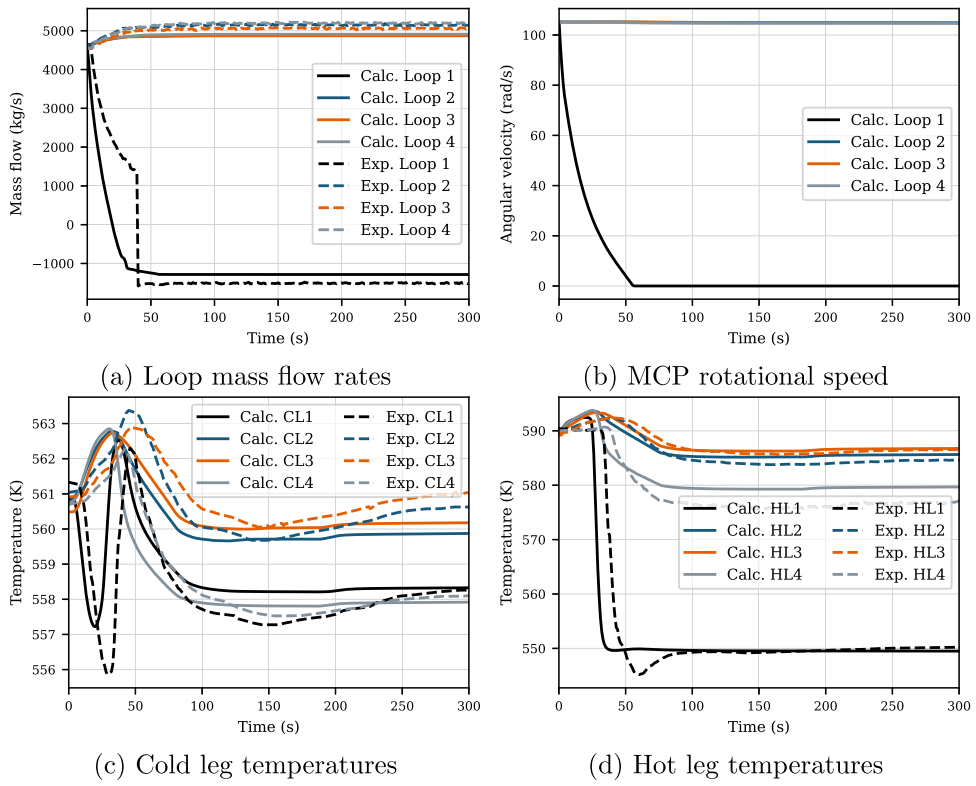

Fig. 20. Ants-TRACE results compared to measurements during Kalinin-3 transient.

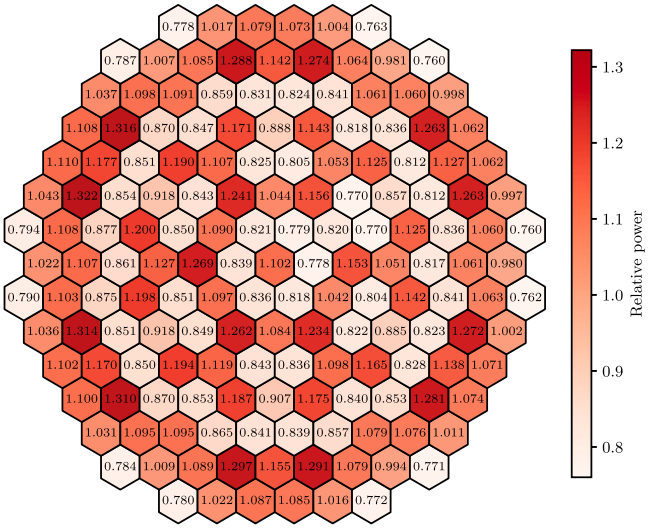

Fig. 21. Ants-TRACE relative radial power distribution at time 300 s in the Kalinin-3 transient.

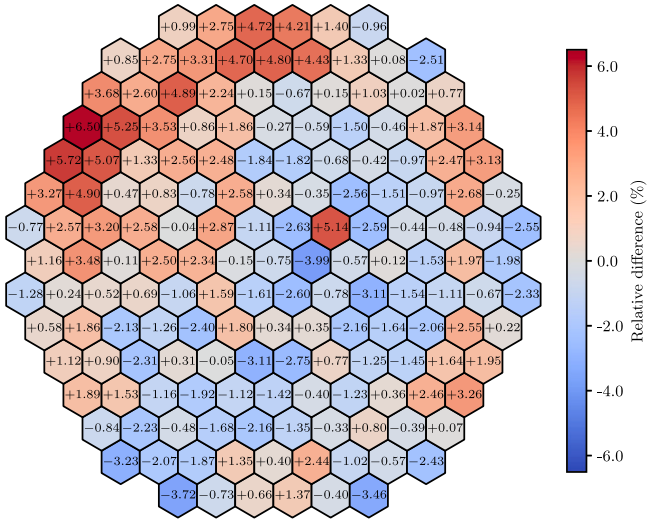

Fig. 22. Relative difference between the radial power distributions of Ants-TRACE and measured data at time 300 s in the Kalinin-3 transient.

line break transient was calculated. Second, Exercise 3 of the Kalinin-3 benchmark consisting of a core-plant simulation of a main coolant pump trip was calculated.

The Ants-TRACE results in the V1000CT-2 benchmark show relatively good agreement with VTT's HEXTRAN-SMABRE code solution. Largest differences in the time history of fission power occur in the pessimistic scenario of the transient, in which the reactor returns to power after scram. The phenomenon is modeled successfully and the deviations remain in the range of other code solutions provided in the benchmark. Some differences between the Ants and HEXTRAN solution arise from the neutronics solution methods, which are significantly different between the codes. The methodology used in Ants to solve the neutron diffusion equation allows more steep flux gradients inside the homogeneous nodes. The group constant files provided in the V1000CT-2 benchmark are used directly in Ants. For HEXTRAN, the group constant files have been pre-processed to another format without information loss. However, the axial and radial reflector nodes defined in the benchmark and used in Ants are replaced in HEXTRAN with equivalent albedo matrices. The albedo matrices are defined at single state points and include only boron feedback correction terms, whereas Ants uses the full interpolation table for the group constant thermal hydraulic feedbacks also in the reflector nodes.

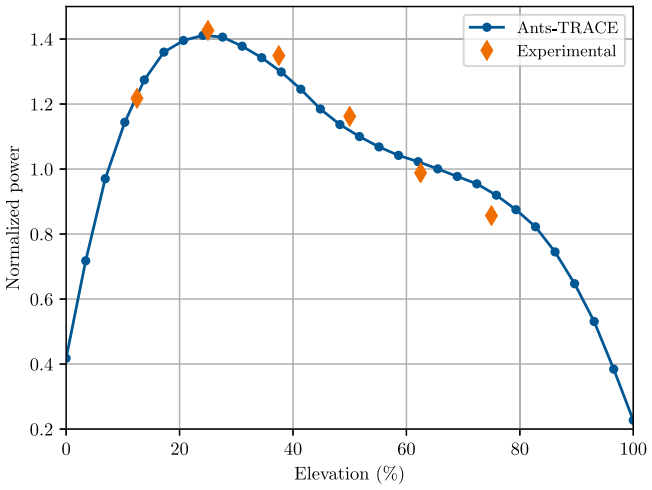

Fig. 23. Relative axial power distribution in the final state (300 s) of the Kalinin-3 transient.

In the Kalinin-3 benchmark, the Ants-TRACE results were compared to measured data from the plant. The Ants-TRACE power distributions in the initial steady state indicated good agreement with the measured data, with the relative difference to measurement being within the range of measurement uncertainty. The only exception occurs in the radial power distribution, in which the difference in power at the position of the replaced fresh fuel assembly slightly exceeds the measurement uncertainty of 5 %. However, similar overestimation of power compared to the measurement in the fresh fuel assembly has occurred in the results of other codes as well (Häkkinen et al., 2020; Ojinnaka et al., 2020).The end-of-transient power distribution contained slightly larger deviations from the measurements in single fuel assemblies. The maximum error of 6.50% exceeds the measurement uncertainty, but can be considered sufficient estimation. The time histories of various parameters indicated correct modeling of the phenomena when compared to the measurement data and the results fall mostly within the measurement uncertainty bounds.

In both exercises, the coupled Ants-TRACE code system performs well in comparison to other code solutions and available real plant data. The results indicate correct implementation of the coupling. The validation process continues with different models and transient scenarios. Ongoing work also includes coupled transient calculations with Ants, TRACE and the fuel performance code SuperFINIX of the Kraken framework. In addition, work on coupled modeling of the thermal hydraulics using TRACE coupled to a porous medium CFD solver OpenFOAM is underway.

CRediT authorship contribution statement

Unna Lauranto: Methodology, Validation, Formal analysis, Writing – original draft, Writing – review & editing, Visualization. **Rebekka Komu:** Conceptualization, Methodology, Validation, Formal analysis, Writing – original draft, Writing – review & editing, Visualization. **Antti Rintala:** Software, Writing – review & editing. **Ville Valtavirta:** Conceptualization, Writing – review & editing, Funding acquisition.

Declaration of competing interest

The authors declare that they have no known competing financial interests or personal relationships that could have appeared to influence the work reported in this paper.

Data availability

Data will be made available on request.

Acknowledgments

This work has received funding from the LONKERO project under The Finnish Research Programme on Nuclear Power Plant Safety 2019–2022 (SAFIR2022) and the DECAPOD project under The National Nuclear Safety and Waste Management Research Programme 2023–2028 (SAFER2028).

References

Apros, 2022. Apros process simulation software. URL: https://www.apros.fi/en/.

Georgieva, E., 2016. Development of a Cross-Section Methodology and a Real-Time Core Model for VVER-1000 Simulator Application (Ph.D. thesis). Karlsruher Institut für Technologie (KIT).

Häkkinen, S., Syrjälahti, E., Rintala, A., 2020. Validation of the Serpent 2-HEXTRAN-SMABRE code sequence in a VVER-1000 coolant transient. J. Nucl. Sci. Technol. 57 (10), 1167–1180. http://dx.doi.org/10.1080/00223131.2020.1773348.

Hirvensalo, M., Rintala, A., Sahlberg, V., 2021. Triangular geometry model for Ants nodal neutronics solver. In: Proceedings of the ANS M&C 2021. Raleigh, North Carolina, USA.

Ivanov, B., Ivanov, K., Groudev, P., Pavlova, M., Hadjiev, V., 2002. VVER-1000 Coolant Transient Benchmark PHASE 1 (V1000CT-1) Vol. I: Main Coolant Pump (MCP) Switching on - Final Specifications. OECD/NEA, NEA/NSC/DOC(2002)6.

Kolev, N., Petrov, N., Donov, J., Angelova, D., Aniel, S., Royer, E., Ivanov, B., Ivanov, K., Lukanov, E., Dinkov, Y., Popov, D., Nikonov, S., 2006. VVER-1000 Coolant Transient Benchmark Phase 2 (V1000CT-2), Vol. II: MSLB Problem - Final Specifications. OECD-NEA, NEA/NSC/DOC (2006)6.

Kolev, N., Spasov, I., Tzanov, T., Royer, E., 2010. VVER-1000 Coolant Transient Benchmark Phase 2 (V1000CT-2): Summary Results of Exercise 2 on Coupled 3D Kinetics/Core-Vessel Thermal Hydraulics and Exercise 3 on Core-Plant MSLB Simulation. OECD-NEA, NEA/NSC/DOC (2010).

Kyrki-Rajamäki, R., 1995. Three-Dimensional Reactor Dynamics Code for VVER Type Nuclear Reactors (Ph.D. thesis). VTT Technical Research Centre of Finland, Espoo (Finland); Helsinki Univ. of Technology, Espoo (Finland).

Leppänen, J., Pusa, M., Viitanen, T., Valtavirta, V., Kaltiaisenaho, T., 2015. The Serpent Monte Carlo code: Status, development and applications in 2013. Ann. Nucl. Energy 82, 142–150. http://dx.doi.org/10.1016/j.anucene.2014.08.024.

Leppänen, J., Valtavirta, V., Rintala, A., Hovi, V., Tuominen, R., Peltonen, J., Hirvensalo, M., Dorval, E., Lauranto, U., Komu, R., 2022. Current status and on-going development of VTT's Kraken core physics computational framework. Energies 15 (3), http://dx.doi.org/10.3390/en15030876.

Leppänen, J., Valtavirta, V., Tuominen, R., Rintala, A., Lauranto, U., 2021. A Finnish district heating reactor: Neutronics design and fuel cycle simulations. In: Proceedings of the International Conference on Nuclear Engineering, Vol. 85246. American Society of Mechanical Engineers, p. V001T04A010.

Ojinnaka, C.A., Zimin, V.G., Strashnykh, V.P., Nikonov, S.P., 2020. Analysis of the Kalinin-3 coolant transient benchmark by SKETCH-N/SKAZKA code system. Ann. Nucl. Energy 147, 107716. http://dx.doi.org/10.1016/j.anucene.2020.107716.

Rintala, A., Lauranto, U., 2022. Time-dependent neutronics model of nodal neutronics program Ants (accepted for publication).

Rintala, A., Sahlberg, V., 2019. Extension of nodal diffusion solver of Ants to hexagonal geometry. Kerntechnik 84 (4), 252–261.

Sahlberg, V., Rintala, A., 2018. Development and first results of a new rectangular nodal diffusion solver of Ants. In: Proceedings of the PHYSOR 2018. Cancun, Mexico.

Syrjälahti, E., Hämäläinen, A., 2006. HEXTRAN–SMABRE calculation of the VVER-1000 coolant transient-1 benchmark. Prog. Nucl. Energy 48 (8), 849–864. http://dx.doi.org/10.1016/j.pnucene.2006.06.007.

Tereshonok, V., Nikonov, S., Lizorkin, M., Velkov, K., Pautz, A., Ivanov, K., 2009. Kalinin-3 Coolant Transient Benchmark - Switching-off of One of the Four Operating Main Circulation Pumps at Nominal Reactor Power. OECD-NEA, NEA/NSC/DOC (2009)5. Final draft.

Tuominen, R., Komu, R., Valtavirta, V., 2022. Coupling of TRACE with nodal neutronics code Ants using the exterior communications interface and VTT's multiphysics driver Cerberus. In: Proceedings of the PHYSOR.

U. S. Nuclear Regulatory Commission, 2020. TRACE V5.0 PATCH 6 THEORY MANUAL - Field Equations, Solution Methods, and Physical Models. Washington, DC.

Valtavirta, V., Peltonen, J., Lauranto, U., Leppänen, J., 2019. SuperFINIX — A flexible-fidelity core level fuel behavior solver for multi-physics applications. In: Proceeding of NENE 2019. Portorož, Slovenia.

Woo, S.W., Cho, N.Z., Noh, J.M., 2001. The analytic function expansion nodal method refined with transverse gradient basis functions and interface flux moments. Nucl. Sci. Eng. 139 (2), 156–173. http://dx.doi.org/10.13182/NSE01-A2229.

Xia, B., Xie, Z., Xian, C., Yao, D., 2006. Flux expansion nodal method for solving static and transient neutron diffusion equations in hexagonal-z geometry. In: Proceedings of the PHYSOR-2006. Vancouver, BC, Canada.